1   **Title:** Elephant megacarcasses increase local nutrient pools in African savanna soils and plants

2

3   Courtney G. Reed[1*], Michelle L. Budny[2], Johan T. du Toit[3,4], Ryan Helcoski[3], Joshua P.

4   Schimel[1], Izak P. J. Smit[5,6], Tercia Strydom[5], Aimee Tallian[3,7], Dave I. Thompson[8,9], Helga van

5   Coller[8,10], Nathan P. Lemoine[2,11], Deron E. Burkepile[1,8*]

6

7   [1]Department of Ecology, Evolution, and Marine Biology, University of California, Santa

8   Barbara, CA, USA

9   [2]Department of Biological Sciences, Marquette University, Milwaukee, WI, USA

10   [3]Department of Wildland Resources, Utah State University, Logan, UT, USA

11   [4]Institute of Zoology, Zoological Society of London, London, England, UK

12   [5]Scientific Services, South African National Parks, Skukuza, South Africa

13   [6]Sustainability Research Unit, Nelson Mandela University, George, South Africa

14   [7]Norwegian Institute for Nature Research, Høgskoleringen 9 Trondheim, 7485 Norway

15   [8]South African Environmental Observation Network (SAEON), Ndlovu Node, Phalaborwa,

16   South Africa

17   [9]Unit for Environmental Sciences and Management, Potchefstroom Campus, North West

18   University, Potchefstroom, South Africa

19   [10]The Expanded Freshwater and Terrestrial Environmental Observation Network (EFTEON),

20   Kimberley 8306, South Africa

21   [11]Department of Zoology, Milwaukee Public Museum, Milwaukee, WI, USA

22

23   *Corresponding authors: Courtney Reed, courtneyreed@ucsb.edu, Deron Burkepile,

24   dburkepile@ucsb.edu

Abstract

African elephants (*Loxodonta africana*) are the largest extant terrestrial mammals, with bodies containing enormous quantities of nutrients. Yet we know little about how these nutrients move through the ecosystem after an elephant dies. Here, we investigated the initial effects (1-26 months postmortem) of elephant megacarcasses on savanna soil and plant nutrient pools in Kruger National Park, South Africa. We hypothesized that: (H1) elephant megacarcass decomposition would release nutrients into soil, resulting in higher concentrations of soil nitrogen (N), phosphorus (P), and micronutrients near the center of carcass sites; (H2) carbon (C) inputs to the soil would stimulate microbial activity, resulting in increased soil respiration potential near the center of carcass sites; and (H3) carcass-derived nutrients would be absorbed by plants, resulting in higher foliar nutrient concentrations near the center of carcass sites. To test our hypotheses, we identified 10 elephant carcass sites split evenly between nutrient-poor granitic and nutrient-rich basaltic soils. At each site, we ran transects in the four cardinal directions from the center of the carcass site, collecting soil and grass (*Urochloa trichopus,* formerly *U. mosambicensis*) samples at 0, 2.5, 5, 10, and 15 m. We then analyzed samples for CNP and micronutrient concentrations and quantified soil microbial respiration potential. We found that concentrations of soil nitrate, ammonium, $\delta^{15}N$, phosphate, and sodium were elevated closer to the center of carcass sites (H1). Microbial respiration potentials were positively correlated with soil organic C, and both respiration and organic C decreased with distance from the carcass (H2). Finally, we found evidence that plants were readily absorbing carcass-derived nutrients from the soil, with foliar %N, $\delta^{15}N$, iron, potassium, magnesium, and sodium significantly elevated closer to the center of carcass sites (H3). Together, these results indicate that elephant megacarcasses release ecologically consequential pulses of nutrients into the soil

48   that influence soil microbial activity and are absorbed by plants into the above-ground nutrient

49   pools. These localized nutrient pulses may drive spatiotemporal heterogeneity in plant diversity,

50   herbivore behavior, and ecosystem processes.

Sect. 1 Introduction

Living animals affect nutrient flows through ecosystems (Schmitz et al. 2018), but we have only recently acknowledged that the nutrients from animal carcasses could also influence ecosystem processes (Barton et al. 2013; Monk et al. 2024). In marine ecosystems, whale carcasses function as unique hotspots of nutrient cycling, biodiversity, and ecosystem processes (Roman et al. 2014). In terrestrial systems, mass mortality events (e.g., wildebeest, cicadas) create nutrient hotspots (Yang, 2004; Subalusky et al. 2020), while individual small and medium-sized carcasses release pulses of nutrients into the soil (Town, 2000; Barton et al. 2016; Olea et al. 2019). Yet, terrestrial ecosystem ecology lacks knowledge about the role of megacarcasses (carcasses of animals such as elephants and rhinoceros that are >1000 kg at death) as potential drivers of spatiotemporal heterogeneity in nutrient cycling and ecosystem processes. Importantly, these megacarcasses may be functionally different than smaller carcasses due to the extraordinarily high concentration of nutrients and residence time of the decomposing animal (see reviews by Barton et al. 2013; Barton, 2016; Barton & Bump 2019). This question around the role of megacarcasses is particularly relevant given the megaherbivore losses that occurred during the Pleistocene extinctions and that are still occurring today (Ripple et al. 2015). We are only beginning to understand how the 'extinction aftershock' of losing the largest species impacts ecosystems (Owen-Smith, 1989; Flannery, 1990), and no study has yet investigated how the loss of megacarcasses might influence the dynamics of terrestrial ecosystems (Doughty et al. 2013; Doughty et al. 2016).

We can only evaluate the importance of terrestrial megacarcasses for nutrient cycling in ecosystems where megaherbivores still exist, such as African savannas. The African savanna elephant (*Loxodonta africana*) is the largest extant land animal and is known for its key

5

74 ecological effects in savannas while alive (e.g., dispersing seeds, creating plant refuges,

75 preventing woody encroachment) (Skarpe et al. 2004; Asner et al. 2009; Campos-Arceiz &

76 Blake, 2011; Coverdale et al. 2016; Guy et al. 2021). Yet, the elephant's large body mass may

77 mean that it also has an outsized impact in these ecosystems even after death. A 4000-kg

78 elephant megacarcass likely represents ~2000 kg carbon (C), ~300 kg nitrogen (N), and ~125 kg

79 phosphorus (P) deposited in the savanna landscape (estimated from stoichiometry of elephants

80 and other mammals in Sterner & Elser, 2002). The N deposition from one elephant megacarcass

81 (in a 700 m^2 impact zone assuming a 15 m disturbance radius) is roughly equivalent to the N

82 delivered to 10,000 m^2 of savanna from ~100 years from atmospheric deposition (Mphepya et al.

83 2006).

84   If megacarcasses provide large nutrient pulses, then they likely create hotspots of

85 important below- and aboveground processes. Belowground, soil respiration and organic matter

86 decomposition might increase with nutrient inputs from carcasses (Risch et al. 2020).

87 Concentrations of C, N, P, and potassium (K) are often elevated near carcasses of medium-sized

88 animals (e.g., bison, moose, kangaroo, vicuña) (Towne, 2000; Bump et al. 2009a; Macdonald et

89 al. 2014; Risch et al. 2020; Monk et al. 2024), and nutrients such as P and calcium (Ca) continue

90 leaching from bones even after soft tissues have been consumed or degraded (Coe, 1978; Keenan

91 & Beeler, 2023). Aboveground, plant growth in African savannas is limited by nutrient

92 availability, most commonly N and P (Ries & Shugart, 2008; Pellegrini, 2016), and

93 micronutrients such as sodium (Na) and potassium (K) may co-limit plant productivity as well

94 (Epron et al. 2012; Chen et al. 2024). Thus, the large influx of nutrients released from

95 megacarcasses might increase the mobilization of nutrients by plants, potentially increasing

96 nutrient accessibility for vertebrate and invertebrate herbivores (Yang, 2008; Grant & Scholes,

97   2006; Anderson et al. 2010; Joern et al. 2012). Indeed, carcasses of smaller vertebrates (e.g.,

98   salmon, deer) can increase the proportions of nitrogen and $\delta^{15}N$ (an indicator of animal-driven N)

99   in plants within just a few months postmortem (Hocking & Reynolds, 2012; van Klink et al.

100 2020).

101   To assess the effects of megacarcasses on local nutrient pools (Figure 1), we measured

102 the initial contributions of elephant carcasses (1-26 months postmortem) to soil and plant

103 nutrients in the Kruger National Park (KNP), South Africa. Further, we examined the effects of

104 elephant carcasses on the two main soil types in KNP: sandy, relatively nutrient-poor granitic

105 soils and clayey, relatively nutrient-rich basaltic soils (Venter et al. 2003). At each site, we ran

106 transects in each cardinal direction from the center of the site where an elephant died, collecting

107 samples of soil and a palatable grass species (*Urochloa trichopus*) at 0, 2.5, 5, 10, and 15 m. We

108 then analyzed soil samples for CNP and micronutrient content, quantified soil microbial

109 respiration potential, and measured %N, $\delta^{15}N$, and macro- and micronutrient content in grass

110 tissue. We hypothesized that: (H1) elephant megacarcass decomposition would release nutrients

111 into soil, resulting in higher concentrations of soil N, P, and micronutrients near the center of

112 carcass sites; (H2) C inputs to the soil would stimulate microbial activity, resulting in increased

113 soil respiration potential near the center of carcass sites; and (H3) carcass-derived nutrients

114 would move from soil into plants, resulting in higher foliar nutrient concentrations near the

115 center of carcass sites. We predicted that enrichment effects from megacarcasses would be

116 greater on sites with fresher carcasses relative to older carcasses and on nutrient-poor granitic

117 sites compared to nutrient-rich basaltic sites.

118

119 **Sect. 2 Methods**

2.1 Study system and sample collection

We performed this research in the southern part of the Kruger National Park (KNP), South Africa (24.996 S, 31.592 E, ~275m elevation). The two dominant soil types in KNP are granitic soils (Inceptisols) and basaltic soils (Versitols or Andisols) (Khomo et al. 2017). The clay-rich basaltic soils have relatively large surface area, enabling them to retain larger quantities of water than granitic soils, which drain water more quickly and therefore are lower in water-soluble nutrients (Buitenweref, Kulmatiski, & Higgins, 2014; Rughöft et al. 2016). The landscape of KNP is a mix of savanna grasslands and broadleaf woodlands, with an overstory dominated by trees from the genus *Combretum* (red bushwillow, *C. apiculatum*; russet bushwillow, *C. hereroense*; leadwood, *C. imberbe*) and trees formerly known as acacias (knobthorn, *Senegalensis nigrescens*; umbrella thorn, *Vachellia tortillis*). The park hosts a full suite of African savanna animals, including ~30,000 elephants (*Loxodonta africana*) (Coetsee & Ferreira, 2023), with a mortality rate of ~2% (~600 elephants per year). The targeted region of KNP has a high density of scavengers and predators, including white-backed vultures (*Gyps africanus*), spotted hyenas (*Crocuta crocuta*), and lions (*Panthera leo*) (Owen-Smith & Mills, 2007).

During the wet season in March 2023, we identified ten elephant carcass sites (1-26 months postmortem), five on relatively nutrient-rich basaltic soil and five on nutrient-poor granitic soil. KNP section rangers provided precise GPS locations of where elephant carcasses had been found. Most elephants died of old age, illness, injury, or, in the case of one young bull, fighting over territory. Carcass sites were recognizable *in situ* by a persistent bonefield, undigested gut contents, and an absence of herbaceous vegetation. At each site, we hammered a rebar post into the center of the megacarcass disturbance and ran 15 m transects out from the

143 post in each of the four cardinal directions. We collected green leaf material from *U. trichopus,* a

144 common and abundant palatable grass species, and used an auger to collect soil samples to a

145 depth of 10 cm at five points along each transect (0.5, 2.5, 5, 10, and 15 m) (Bump, Peterson, &

146 Vucetich, 2009; Holdo & Mack, 2014; Gray & Bond, 2015; Monk et al. 2024). We treated the

147 10-15m distances as representative of background concentrations of nutrients based on pilot data

148 showing that the effect of elephant carcasses on soil nutrient concentrations was undetectable at

149 this distance away from the carcass site, similar to studies on the carcasses of other large

150 vertebrates (e.g., Towne, 2000; Bump et al. 2009). We pooled and homogenized the samples to

151 yield one composite leaf and one composite soil sample per sampling distance from each carcass

152 site. Soil samples were sieved in a 5-mm metal sieve which was cleaned in between samples

153 with 70% ethanol. Soil samples were stored in a cooler during fieldwork. On the day they were

154 collected, we used 5 g of each soil sample for soil respiration measurements (described below).

155 The rest of each sample was placed in a plastic bag on the day of collection and stored in a -20°C

156 freezer for up to 1 month; samples were stored in coolers with ice blocks during the transition

157 from the freezer at the field site to the lab for analysis. We chose to freeze samples rather than

158 storing at room temperature based on literature demonstrating that the impacts of freezing on soil

159 nitrate and ammonium concentrations are fairly minimal, except in specific cases of high soil

160 acidity or peaty soils that were not present at our field site (Esala, 1995; Turner & Romero, 2009;

161 Sollen-Norrlin & Rintoul-Hynes, 2024). Leaf samples were stored in paper bags at room

162 temperature until dried for analyses (see below).

163

164 **2.3 Hypothesis testing**

165   We tested our first hypothesis that elephant carcass decomposition would release nutrients into

166   the soil by performing soil nutrient analyses. We sent 250 g of each soil sample to Eco-Analytica

167   laboratory at the North-West University in Potchefstroom, South Africa for measurements of soil

168   concentrations of ammonium $[NH_4]^+$, nitrate $[NO_3]^-$, phosphate $[PO_4]^{3-}$, and plant-available P.

169   Samples were air-dried and sieved through < 2mm mesh prior to chemical analysis. Plant-

170   available P was extracted from 4 g of soil and 30 ml extraction fluid (1:7.5 ratio) using an acid–

171   fluoride solution (P Bray-1) (FAO, 2021), measured colorimetrically using a Systea

172   EasyChem200 analyser, and expressed as mg/kg. The detection limit was 0.5 mg/kg, and plant

173   available P measurements <0.5 mg/kg were replaced with half the detection limit (0.25 mg/kg)

174   (Croghan & Egeghy, 2003). Water-soluble nitrate and phosphate anions were extracted from

175   volume on volume 100 mg soil and 200 ml deionized water (Sonneveld & van den Ende, 1981),

176   analyzed by ion chromatography on a Metrohm 930 Compact Flex System, and measured as

177   mg/L. Ammonium (also 1:2 water extract) was analyzed colorimetrically using a Systea

178   EasyChem200 analyzer and measured as mg/L. Detection limits for soil ions were 0.01 mg/L,

179   and soil ion concentrations measured as <0.01 mg/L were replaced with half the detection limit

180   (0.005 mg/L). To convert the nitrate, ammonium, and phosphate units from mg/L to mg/kg, we

181   multiplied by 2, based on the 1:2 soil to water extraction ratio.

182   To determine whether soil micronutrients were distinct and elevated at the center of

183   carcass sites relative to soil further from the center, we measured concentrations of sodium (Na),

184   magnesium (Mg), iron (Fe), calcium (Ca), potassium (K), and phosphorus (P). Air-dried and

185   sieved (>2 mm) soil samples, weighed to 0.2 g, were microwaved in 9 ml 65% nitric acid

186   (HNO_3) and 3 ml 32% hydrochloric acid (HCl) according to EPA 3051b in a Milestone, Ethos

187   microwave digester with UP, Maxi 44 rotor. A period of 20 minutes allowed the system to reach

188 1800 MW at a temperature of 200 °C which was maintained for 15 minutes. After cooling, the

189 samples were brought up to a final volume of 50 ml and analyzed on an Agilent 7500 CE ICP-

190 MS fitted with CRC (Collision Reaction Cell) technology for interference removal. The

191 instrument is optimized using a solution containing Li, Y, Ce, and Tl (1 ppb) for standard low-

192 oxide/low interference levels ($\leq$ 1.5%) while maintaining high sensitivity across the mass range.

193 The instrument was calibrated using ULTRASPEC® certified custom mixed multi-element stock

194 standard solutions containing all the elements of interest (De Bruyn Spectroscopic Solutions,

195 South Africa). Calibrations spanned the range of 0 – 30 ppm for the mineral elements Ca, Mg,

196 Na, and K and 0 – 0.3 ppm for the rest of the trace elements. Elemental concentrations were

197 expressed as mg/kg.

198   Finally, to determine whether elevated N levels in soils were derived from the carcass, we

199 sent 10 g of each sample to the BIOGRIP laboratory within the Central Analytical Facility at

200 Stellenbosch University for measurements of soil %N and δ^{15}N, obtained using a Vario Isotope

201 Select Elemental Analyzer connected to a thermal conductivity detector and an Isoprime

202 precisions isotope ratio mass spectrometer (IRMS). Samples were oven-dried at 60°C for 48

203 hours and milled to a fine powder using a Retsch MM400 mill (Germany). The powdered

204 samples were weighed (2 – 60 mg) prior to combustion at 950°C. The gasses were reduced to N_2

205 (undiluted) in the reduction column, which was held at 600°C. A high organic carbon (HOC) soil

206 standard (0.52 ± 0.02 %N), along with two international reference standards (USGS40 (δ^{15}N -

207 4.52% AIR) and USGS41 (δ^{15}N +47.57% AIR)) were used for calibration. The N elemental

208 content was expressed relative to atmospheric N as N_2 δ^{15}NAIR (‰). The quantification limit for

209 δ^{15}N on the IRMS is 1 nA (nanoAmp), and the quantification limit for %N is 0.06%. The

210   precision for %N was 0.02% and for $\delta^{15}N$ is ±0.11%, determined using the HOC standard, which

211   was run multiple times throughout the analysis.

212   To test our second hypothesis that nutrient inputs to the soil would stimulate microbial

213   activity, we measured soil organic C, water content, and microbial respiration potential. We sent

214   10 g of each sample to the BIOGRIP laboratory for measurements of soil organic C using a

215   Vario TOC Cube (Elementar, Germany). Samples (dried and milled as above) were weighed (10

216   – 60 mg), acidified using 10% HCl to remove the total inorganic C (carbonates), and dried

217   overnight at 60°C. All samples were analyzed through combustion at 950°C. The released CO_2

218   was measured by a non-dispersive infrared (NDIR) sensor. A high organic C (7.45 ± 0.14 %C)

219   soil standard from Elemental Microanalysis Ltd (UK) was included during the analysis. The

220   quantification limit for %C is 0.14%. The precision for the %C was 0.09% and was determined

221   using the low organic C (LOC) standard (1.86 ± 0.14 %C), which was run multiple times

222   throughout the analysis.

223   To quantify soil respiration and water content, we used an incubation method (Lemoine

224   et al. 2023) in which 5 g (± 0.2 g) of each sample was placed into a 100 ml clear glass bottle,

225   sealed, and flushed with CO_2-free air. Following flushing, we incubated the bottles for one hour

226   at 25°C. We then recorded CO_2 concentrations using an LI-850 CO_2/H_2O infrared gas analyzer.

227   After soil respiration measurements, we determined sample dry weight by drying each sample at

228   60°C for 24-48 hours until stable mass was achieved. We subtracted dry weight from starting

229   weight to obtain soil water content. Finally, we used the dry weights and the Ideal Gas Law to

230   standardize all respiration measurements to CO_2 $\mu g\ h^{-1} g$ dry $soil^{-1}$.

231   To test our third hypothesis that carcass-derived nutrients would be incorporated by

232   plants, we measured foliar nutrient concentrations in *U. trichopus*. Two grams of each dried leaf

233   sample was sent to the BIOGRIP laboratory for preparation and measurements of %N and $\delta^{15}N$

234   via stable isotope analysis as described above. A Sorghum flour standard (1.47 ± 0.25 %N) from

235   Elemental Microanalysis Ltd (UK) was used for calibration, along with two international

236   reference standards (USGS40 and USGS41). The quantification limit for $\delta^{15}N$ on the IRMS is 1

237   nA, and the quantification limit for %N is 1.3%. The precision for the %N was 0.02% and for

238   $\delta^{15}N$ is ±0.08‰. Limits were determined using the sorghum flour standard, which was run

239   multiple times throughout the analysis. Additionally, we sent 5 g per sample to Cedara

240   Analytical Services Laboratory to quantify micronutrients in grass tissue (P, Na, Mg, K, Ca, and

241   Fe) using Inductively Coupled Plasma Optical Emission Spectroscopy (ICP-OES 5800, Agilent,

242   USA). Samples were dried (110°C overnight) and milled to a fine powder. Subsamples (0.5 g)

243   were ashed at 450°C for 4 hours, and the ash was re-wet using 2 mL conc. HCl (32%). Samples

244   were evaporated to dryness then re-suspended in 25 mL 1M HCl before filtering. Lastly, the

245   filtrate was diluted with de-ionized water in a ratio of 5:20 filtrate to water. To calibrate the ICP-

246   OES, solutions containing known amounts of each element were measured (10-20 ppm for Na

247   and C, 200-1500 ppm for Fe, 0.5-3.75% for K, and 0.125-0.5% for P), prepared from 1000 ppm

248   primary single standards. At three of the ten sites, we did not find sufficient plant material at the

249   central point for analysis, resulting in a sample size of N = 7 for the center (distance = 0.5m)

250   measurement for leaf nutrient analyses.

251   To test whether each response variable for the three hypotheses was significantly

252   associated with soil type and/or distance from the carcass center, we performed a model selection

253   procedure. For each response variable, we ran five generalized linear mixed models using the

254   gamma family (link = log) in the package *lme4* (Bates et al. 2015): (*i*) soil type + distance + soil

255   type × distance interaction, (*ii*) soil type + distance, (*iii*) soil type, (*iv*) distance, and (v) a null

256   model indicating no significant difference in slope or intercept after accounting for carcass site.

257   All models included carcass site as a random effect to account for individual variation. Each

258   model included 50 observations (10 sites x 5 distances per site). For samples in which the

259   nutrient level was listed as 0 or undetectable, we accounted for the uncertainty by using half the

260   detection level as described above. The narrow distribution of ages (1-26 months since death)

261   with the sample size of N = 10 sites made testing for the effect of age challenging, so we did not

262   include carcass age in the models. We compared the models for each response variable using

263   Akaike Information Criterion (AICc). Models with a ΔAICc ≤ 2 were considered roughly

264   equivalent in fit (Burnham and Anderson, 2002).

265   In addition to these models, for our second hypothesis we regressed soil respiration

266   potential against soil organic C, expecting that the two would be positively correlated. We ran a

267   generalized linear mixed model with soil respiration potential as the response variable. The

268   model included soil organic C + distance + soil type, with carcass site as a random effect. We did

269   not include an interaction with soil type in this model due to sample size restrictions. Respiration

270   potential and organic C were both log-transformed to achieve normality.

271   To determine whether leaf and soil micronutrient composition differed with distance and

272   soil type, we ran permutational analysis of variance (perMANOVA) in *vegan* (Oksanen et al.

273   2022). We ran the same model separately for soil and leaf micronutrient composition (soil type +

274   distance). To determine which micronutrients contributed most to compositional differences

275   across distances and soil types, we calculated samplewise Bray-Curtis dissimilarity and

276   performed principal component analysis. We also tested for differences in variance in

277   micronutrient composition across distances and soil types using "betadisper" in *vegan* (Oksanen

278   et al. 2022). We ran linear models to test for correlations between leaf and soil concentrations of

279   each micronutrient. Each model included distance as a covariate and site as a random effect.

280   Finally, to test the impact of carcass age on key soil metrics, we ran exponential decay

281   functions for soil ammonium, nitrate, phosphate, and respiration verses carcass age for samples

282   from the center of the carcass site (0.5m sampling location). We also performed a t-test to verify

283   that there was no difference in mean carcass age across soil types.

284   All statistical analyses were performed in R version 4.2.1 (R Core Team, 2022).

285

286   **Sect. 3 Results**

287   **3.1 Hypothesis 1: Effects of megacarcasses on soil nutrient pools**

288   We found partial support for our first hypothesis that soil N and P concentrations would be

289   higher closer to the center of carcass sites (Table S1). Soil %N (Figure 2A) was overall greater in

290   basaltic soils, and it decreased with distance from the carcass site on granitic soils. Soil nitrate

291   (Figure 2B) decreased with distance from the carcass site but did not differ between soil types.

292   Ammonium (Figure 2C) also decreased with distance, but only in granitic soils. $\delta^{15}N$ (Figure 2D)

293   was greater in granitic soils and decreased with distance in both soil types, indicating that the

294   proportion of animal-sourced N in the soil was greater near the center of the carcass site. Soil

295   phosphate, plant available P, and mineral P (Figure 2E-G) all exhibited significant soil × distance

296   interactions. Phosphate (Figure 2E) was highly elevated at the center of carcass sites and

297   decreased steeply with distance, but only in granitic soils. Plant-available P (Figure 2F)

298   decreased with distance in both soil types, but the effect was strongest in granitic soils. Finally,

299   mineral P (Figure 2G) was greater in basaltic soils, and there was a small decrease with distance

300   in granitic soils but not in basaltic soils.

301   Contrary to our first hypothesis, soil micronutrient composition did not differ

302   significantly with distance from the carcass center; nor did most individual micronutrients (Table

303   S1). The perMANOVA results showed that soil micronutrient composition did not differ

304   significantly with distance ($R^2 = 0.00$, $F_{4,44} = 0.0$, $P = 1.000$) (Figure S2A), but it did differ

305   significantly with soil type ($R^2 = 0.71$, $F_{1,44} = 108.8$, $P = 0.001$) (Figure S2B). There was no

306   significant difference in variance with distance ($F_{4,45} = 0.0$, $P = 0.996$) or soil type ($F_{1,48} = 2.6$, P

307    $= 0.115$). Principal components analysis showed that dimension 1 explained 53.6% of the

308   variation between soil types and was driven primarily by differences in Mg, Ca, and Fe.

309   Dimension 2 explained 25.9% of variation and was driven primarily by differences in K. Soil Na

310   (Figure S3A) was marginally greater in granitic soils and decreased with distance from the

311   carcass, with the effect greater in granitic soils. Soil K (Figure S3B) was greater in basaltic soils

312   and decreased marginally with distance. Soil Fe, Mg, and Ca (Figure S3C-E) were greater in

313   basaltic soils, with minimal effects of distance.

314

315   **3.2 Hypothesis 2: Effects of megacarcasses on soil carbon and respiration**

316   Consistent with our second hypothesis, soil respiration potential was marginally positively

317   correlated with soil organic carbon concentration and decreased significantly with distance but

318   did not differ with soil type (Figure 3). We found no evidence for differences in soil water

319   content (Figure S4A) or soil pH (Figure S4B) with distance or soil type. In both cases, the null

320   ranked among the set of top models (Table S1).

321

322   **3.3 Hypothesis 3: Effects of megacarcasses on plant nutrient pools**

16

323   Consistent with our third hypothesis, we found elevated foliar nutrient concentrations in *U.*

324   *trichopus* at elephant carcass sites. Leaf %N (Figure 4A) and δ^{15}N (Figure 4B) both decreased

325   with distance from the carcass center. δ^{15}N exhibited a significant soil × distance interaction in

326   which it was overall greater in basaltic soils, but the difference between the two soil types was

327   greater closer to the carcass site. Foliar P was greater in basaltic soils and decreased only

328   marginally with distance in the granite soils. Finally, the foliar N:P ratio was greater in granitic

329   soils and decreased with distance in the basaltic soils.

330   Leaf micronutrient composition did not differ significantly with distance ($R^2 = 0.13$, $F_{4,40}$

331   $= 1.9$, $P = 0.062$; Figure S5A) but did differ with soil type ($R^2 = 0.17$, $F_{1,40} = 9.7$, $P = 0.001$;

332   Figure S5B). There was no significant difference in variance with distance ($F_{4,41} = 0.5$, $P =$

333   0.713) or soil type ($F_{1,44} = 1.9$, $P = 0.173$). Dimension 1 explained 42.8% of the variance across

334   soil types and was primarily driven by Mg, Na, and P. Dimension 2 explained 26.6% of the

335   variance and was driven mainly by K, Ca, and Fe. Foliar Na (Figure S6A) and Mg (Figure S6B)

336   were both greater in basaltic soils and decreased with distance from the carcass center. Foliar K

337   (Figure S6C) and Fe (Figure S6D) both decreased with distance as well but did not differ with

338   soil type. The null model was in the top set for foliar Ca, indicating no significant relationship

339   between foliar Ca concentrations and soil type or distance from the carcass center. Individual

340   micronutrients (K, Ca, Mg, Fe) were not correlated between leaf and soil samples, with the

341   exception of Na (Table S3).

342

343   **3.4 Effects of carcass age on soil ions and respiration potential**

344   Soil ammonium ($\alpha = 0.018$, $P < 0.001$), phosphate ($\alpha = 0.023$, $P < 0.001$), and respiration

345   potential ($\alpha = 0.058$, $P < 0.001$) all decreased significantly with carcass age (Figure 5A-C). The

17

346 exponential decay model for nitrate failed to converge due to an outlier with extremely high soil

347 nitrate (1454 mg/kg) at 258 days postmortem (Figure 5D). We ran a t-test to test for a difference

348 in mean carcass age between soil types and found no significant difference between the two

349 groups ($P = 0.294$).

350

351 **Sect. 4 Discussion**

352 Here, we show that elephant megacarcasses influence soil and foliar nutrients during at least the

353 first two years following mortality. Consistent with our hypotheses, soil nitrate (Figure 2B),

354 ammonium (Figure 2C), $\delta^{15}N$ (Figure 2D), and P (Figure 2E-F) concentrations were all elevated

355 at the center of carcass sites and decreased with distance from the center. Soil %N, nitrate,

356 ammonium, and plant-available P concentrations at the 15m point were consistent with those

357 found in other studies of soil nutrient content in Kruger (Aranibar et al. 2003; Rughöft et al.

358 2016), confirming that the 15m point serves as an effective baseline control in this experiment.

359 Microbial respiration potential was also elevated towards the center of carcass sites and was

360 correlated with the abundance of organic C (Figure 3). Finally, %N (Figure 4A) and $\delta^{15}N$ in a

361 common grass (Figure 4B) were both elevated closer to the centers of carcass sites compared to

362 grass farther from carcasses. Together, these results indicate that carcass-derived nutrients move

363 into soil and subsequently get absorbed by plants over relatively short time scales, cycling

364 essential nutrients such as N from carrion into the soil and then back into aboveground nutrient

365 pools.

366   The initial influx of ammonium from elephant carcasses may have time-dependent

367 impacts on plant abundance at elephant carcass sites. The mean ammonium level at the center of

368 carcass sites (34.8 mg/kg) was higher than the level generally considered toxic to plants (Britto

369   & Kronzucker, 2002). Yet, we found living grass—typically *U. trichopus*—in the center of the

370   carcass site at seven out of ten of our sites (ammonium range 10-172 mg/kg) and at the 2.5m

371   distance for all sites (ammonium range 0-72 mg/kg). The three sites without vegetation in the

372   center had the highest ammonium levels (70-144 mg/kg), suggesting that *U. trichopus* has a

373   higher degree of ammonium tolerance than some sympatric grass species but may still be limited

374   by the high ammonium levels at the centers of these three relatively fresh carcass sites. However,

375   the recentness of the disturbance from the carcass likely also plays a role in determining plant

376   abundance near the center of the carcass. Because of the elephant carcass site age distribution,

377   (mean 350 days postmortem; range 24-811 days), this study may not have captured the full

378   impact of ammonium release from carcasses during the early stages of decomposition. Soil

379   ammonium spiked early and decreased rapidly (Figure 5A), and future research on carcasses

380   within the first few weeks postmortem would enhance our understanding of these early nutrient

381   dynamics.

382   Soil nitrate (Figure 2B) and soil respiration potential (Figure 3) were also elevated near

383   the center of carcass sites, indicating higher activity rates for nitrifying bacteria and heterotrophic

384   microbes (Prosser, 2011). These results are consistent with other work on carrion, where

385   microbial activity tends to be greater in soils near carcasses as compared to surrounding soil

386   (Bump et al. 2009b). However, carcass effects on soil microbial respiration exhibit a high degree

387   of intra-system variation (Risch et al. 2020), and the potentially short window during which

388   increased respiration occurs may make capturing these variations challenging. For example, soil

389   respiration potential at the center of the three youngest carcass sites was on average 2x higher

390   than the seven older sites (18.43 and 9.62 μg CO_2 per hour per gram of dry soil, respectively;

391   Figure 5D). Thus, the impact of increased organic C on soil microbial processes may be

392   relatively short lived and only last a matter of months (Keenan et al. 2018; Keenan, Schaeffer, &

393   DeBruyn, 2019). These trends are consistent with soil ammonium and phosphate, both of which

394   are highest at the youngest carcass sites (<200 days postmortem; Figure 5A-B). Soil microbial

395   respiration rate is also highly elevated early on, but it decreases at a faster rate over time than soil

396   ions (Figure 5C). Thus, soil dynamics during the first several months after death may play a

397   crucial role in determining the long-term impacts of megacarcasses on savannas and therefore

398   provides a promising avenue for future research.

399   Elevated soil phosphate (Figure 2E) and plant-available P (Figure 2F) at the center of

400   carcass sites were also consistent with expectations from the literature (Bump et al. 2009a;

401   Parmenter & MacMahon, 2009). However, elevated P levels in soil did not translate to elevated

402   P in grass leaves (Figure 4C), which could suggest a lag between trends in soil and plants that is

403   longer for P than for N. This lag could occur because phosphate easily forms chemical bonds

404   with other soil ions (e.g., iron and aluminum in acidic soils and calcium in basic soils). Nitrate

405   does not form these bonds and therefore has greater water solubility and mobility in soils and

406   may be more readily taken up by plants (Wiersum, 1962; Arai & Sparks, 2007). However, it is

407   also possible that P limitation in Kruger is not as strong as it is in some other African savanna

408   systems (Pellegrini, 2016). The foliar N:P ratios measured in this experiment were higher closer

409   to the center of the carcass site (median 9.38 at 0 m and 4.83 at 15 m), indicating that N

410   limitation may be relatively stronger further from the carcass site, and P limitation may be

411   relatively stronger closer to the center (Figure 4D, Table S2). These relatively high foliar N:P

412   ratios at the center of carcass sites are similar to those found in N fertilization studies in Kruger

413   (Craine et al. 2008), further supporting the idea that the influx of N from megacarcasses may

414   shift the soil from relatively more N limited to more P limited.

415   The elevated plant-available P at the center of carcass sites likely came primarily from

416   phosphate released from decomposing tissue (Yong et al. 2019). Bone decomposition, which is

417   also likely a major source of P from animal carcasses (Subalusky et al. 2020), occurs over long

418   time scales (Coe, 1978; Subalusky et al. 2020) and therefore should result in the slow release of

419   P and a gradual decrease in the N:P ratio (Parmenter & MacMahon, 2009; Quaggiotto et al.

420   2019). Indeed, initial inorganic N influxes to the Mara River in Kenya from mass wildebeest die-

421   offs are 10-fold greater than concurrent increases in P, which instead releases slowly over about

422   seven years of bone decomposition (Subalusky et al. 2017). Research following megacarcasses

423   over longer timeframes postmortem is needed to clarify when P from enriched soil is absorbed

424   by plants and at what stage megacarcass bones begin contributing to soil P dynamics. It is also

425   possible that bone dispersal by scavengers may result in less P leaching from bones close to

426   where the elephant died and more P being distributed across the landscape at distances far from

427   the carcass site.

428   The contributions of megacarcasses to soil nutrient pools were strongly associated with

429   soil type. Our results confirmed the previously-established trend that basaltic soils are overall

430   more cation rich than granitic soils, with greater concentrations of P, K, Fe, Mg, and Ca (Figure

431   2G; Figure S3B-E; Gertenbach, 1983; Craine, Morrow, & Stock, 2008; Wigley et al. 2014).

432   However, soil ammonium, $\delta^{15}N$, and phosphate were all higher in the granitic soils towards the

433   center of carcass sites, decreasing steeply to be similar to basaltic soils about 10 m from the

434   carcass center (Figure 2C-E). These results indicate that the impact of organic matter from

435   megacarcasses may be stronger in relatively nutrient-poor and sandy granitic soil compared with

436   nutrient-rich and clayey basaltic soil. We were surprised that grass on basaltic soil did not

437   consistently exhibit greater nutrient concentrations. One potential explanation is that grass may

21

438   primarily be limited by macronutrients like N and P on both soil types (Craine et al. 2008;

439   Holdo, 2013) rather than by micronutrients. Thus, even with increased micronutrient availability

440   their actual uptake may not differ substantially. Studies on ungulate carcasses (e.g., muskoxen,

441   moose, zebra) have shown increased foliar N at carcass sites (Danell et al. 2002; Bump et al.

442   2009b; Turner et al. 2014), but to date there is little research on the flow of micronutrients from

443   carrion to plants and none on the pipeline from megacarcasses to plants. Moreover, it remains to

444   be seen whether increases in foliar N and other nutrients affect herbivory rates at carcass sites

445   and how long such effects may last.

446   The magnitude of nitrogen inputs from megacarcasses, as well as the substantial size and

447   duration of their impact zones, means their impacts on ecosystem processes may be functionally

448   distinct from smaller carrion. Soil nitrate concentrations at elephant carcass sites are orders of

449   magnitude higher than at carcass sites of smaller carrion (e.g., rabbits, white-tailed deer,

450   kangaroo) (Quaggiato et al. 2019; Bump et al. 2009; Barton et al. 2016). Even for large ungulates

451   such as moose, total soil inorganic nitrogen (ammonium + nitrate) at carcass sites is a mean 300

452   mg/kg (Bump, Peterson, & Vucetich, 2009), substantially lower than the mean total soil

453   inorganic nitrogen at elephant carcass sites (2.5m distance; 473 mg/kg). Termite mounds,

454   another long-lasting source of savanna nutrient heterogeneity, have mean soil nitrate

455   concentrations (197 mg/kg) lower than elephant carcass sites, but maximum nitrate

456   concentrations that are on par with them (974 mg/kg) (Seymour et al. 2014), again indicating that

457   elephant carcasses are one of the strongest known individual contributors of soil nitrogen in

458   African savanna ecosystems, which may have important implications for savanna ecology.

459   Indeed, there is evidence that carcass size strongly impacts scavenger food web structure

460   (Moleón et al. 2015; Morris et al. 2023). Moreover, the attraction of animals to carcasses via

461 scavenging, predation, or mourning (Goldenberg & Wittemyer, 2020) could have positive

462 feedbacks on nutrient cycling (Bump, Peterson, & Vucetich, 2009; Monk et al. 2024), which

463 may be magnified by carcass size. Thus, the impacts of megacarcasses on savanna ecosystem

464 processes may be dissimilar to the effects of small carrion and more similar to other more

465 persistent contributors to savanna ecosystem processes, such as termite mounds (Davies et al.

466 2016), cattle bomas (Augustine, 2003), and even mass animal mortality events (Subalusky et al.

467 2017, 2020).

468

469 **Sect. 5 Conclusions**

470 This study is an important first step in understanding the ecological legacies of megacarcasses on

471 savanna ecosystem processes. During the first two years postmortem, elephant carcasses released

472 pulses of nitrogen and phosphate, which influence savanna primary productivity. These nutrients

473 stimulated soil microbial activity and enriched foliar N, and the effects were strongest in

474 nutrient-poor soil, with potential long-term impacts on savanna nutrient heterogeneity. These

475 carcass-derived nutrient hotspots represent a previously unstudied function of megaherbivores on

476 savannas—one that we need to better understand in order to comprehend the full impacts of

477 megaherbivore population declines in modern ecosystems.

478

479 **Data and Code Availability:** Data and computer code are archived on Dryad Digital Repository

480 (https://doi.org/10.5061/dryad.wpzgmsbwm).

481

482 **Author Contributions:** Deron E. Burkepile, Nathan P. Lemoine, Izak P. J. Smit, Tercia

483 Strydom, Aimee Tallian, Johan T. du Toit, Dave I. Thompson, and Joshua P. Schimel conceived

484 the study. Michelle L. Budny, Johan T. du Toit, Nathan P. Lemoine, Joshua P. Schimel, Izak P.

501

502 **References**

503 1. Agbenin, J. O. & Yakubu, S. Potassium-calcium and potatssium-magnesium exchange

504   equilibria in an acid savanna soil from northern Nigeria. *Geoderma*, 136, 542-554,

505   https://doi.org/10.1016/j.geoderma.2006.04.008, 2006.

506   2.   Anderson, T. M., Hopcraft, J. G. C., Eby, S., Ritchie, M., Grace, J. B., & Olff, H. Landscape-

507   scale analyses suggest both nutrient and antipredator advantages to Serengeti herbivore

508   hotspots. *Ecol.,* 91, 1519–1529, https://doi.org/10.1890/09-0739.1, 2010.

509   3.   Aranibar, J. N., Macko, S. A., Anderson, I. C., Potgieter, A. L. F., Sowry, R. & Shugart, H.

510   H. Nutrient cycling responses to fire frequency in the Kruger National Park (South Africa) as

511   indicated by stable isotope analysis. *Isotopes Environ. Health Stud.,* 39, 141-158,

512   https://doi.org/10.1080/1025601031000096736, 2003.

513   4.   Aria, Y. & Sparks, D. L. Phosphate reaction dynamics in soils and soil components: a

514   multiscale approach. *Adv. Agron*., 94, 135-179, https://doi.org/10.1016/S0065-

515   2113(06)94003-6, 2007.

516   5.   Asner, G. P., Levick, S. R., Kennedy-Bowdoin, T., Knapp, D. E., Emerson, R., Jacobson, J.,

517   Colgan, M. S., & Martin, R. E. Large-scale impacts of herbivores on the structural diversity

518   of African savannas. *PNAS*, 106, 4947–4952, https://doi.org/10.1073/pnas.0810637106,

519   2009.

520   6.   Augustine, D. J. Long-term, livestock-mediated redistribution of nitrogen and phosphorus in

521   an East African savanna. *J. Appl. Ecol*., 40, 137-149, https://doi.org/10.1046/j.1365-

522   2664.2003.00778.x, 2003.

523   7.   Barton, P. S., Cunningham, S. A., Lindenmayer, D. B., & Manning, A. D. The role of carrion

524   in maintaining biodiversity and ecological processes in terrestrial ecosystems. *Oecologia*,

525   171, 761–772, https://doi.org/10.1007/s00442-012-2460-3, 2013.

526   8.   Barton, P.S. Carrion Ecology, Evolution, and Their Applications. Edited by: M.E. Benbow,

527   J.K. Tomberlin, A.M. Tarone. CRC Press, Boca Raton, FL, USA. 2016.

528   9. Barton, P. S., McIntyre, S., Evans, M. J., Bump, J. K., Cunningham, S. A., & Manning, A. D.

529   Substantial long-term effects of carcass addition on soil and plants in a grassy eucalypt

530   woodland. *Ecosphere,* 7, e01537, https://doi.org/10.1002/ecs2.1537, 2016.

531   10. Barton, P.S., Bump, J.K. Carrion decomposition. In: Carrion Ecology and Management.

532   Edited by: P.P. Olea, P. Mateo-Tomas, J.A. Sanchez-Zapata. Springer, NY, USA, 101-124,

533   2019.

534   11. Bates, D., Mächler, M., Bolker, B., & Walker, S. Fitting linear mixed-effects models using

535   lme4. *J. Stat. Softw*., 67, 1–48, https://doi.org/10.18637/jss.v067.i01, 2015.

536   12. Britto, D. T., & Kronzucker, H. J. NH_4^+ toxicity in higher plants: a critical review. *J. Plant*

537   *Physiol.,* 159, 567–584, https://doi.org/10.1078/0176-1617-0774, 2002.

538   13. Buitenwerf, R., Kulmatiski, A. & Higgins, S. I. Soil water retention curves for the major soil

539   types of the Kruger National Park. *Koedoe*, 56, a1228,

540   http://dx.doi.org/10.4102/koedoe.v56i1.1228, 2014.

541   14. Bump, J. K., Peterson, R. O., & Vucetich, J. A. Wolves modulate soil nutrient heterogeneity

542   and foliar nitrogen by configuring the distribution of ungulate carcasses. *Ecol.,* 90, 3159–

543   3167, https://doi.org/10.1890/09-0292.1, 2009.

544   15. Bump, J. K., Webster, C. R., Vucetich, J. A., Peterson, R. O., Shields, J. M., & Powers, M.

545   D. (2009). Ungulate carcasses perforate ecological filters and create biogeochemical hotspots

546   in forest herbaceous layers allowing trees a competitive advantage. *Ecosyst.,* 12, 996–1007,

547   https://doi.org/10.1007/s10021-009-9274-0, 2009.

548   16. Burnham, K. P. & Anderson, D. R. Model Selection and Multimodel Inference. Springer

549   New York, NY. http://doi.org/10.1007/b97636, 2002.

550   17. Campos-Arceiz, A., & Blake, S. Megagardeners of the forest – the role of elephants in seed

551   dispersal. *Acta Oecol.*, 37, 542–553, https://doi.org/10.1016/j.actao.2011.01.014, 2011.

552   18. Chen, J., Gutjahr, C., Bleckmann, A., & Dresselhaus, T. Calcium signaling during

553   reproduction and biotrophic fungal interactions in plants. *Mol. Plant,* 8, 595–611,

554   https://doi.org/10.1016/j.molp.2015.01.023, 2015.

555   19. Chen, B., Fang, J., Piao, S., Ciais, P., Black, T. A., Wang, F., Niu, S., Zeng, Z. & Luo, Y. A

556   meta-analysis highlights globally widespread potassium limitation in terrestrial ecosystems.

557   *New Phytologist,* 241, 154-165, https://doi.org/10.1111/nph.19294, 2024.

558   20. Coe, M. The decomposition of elephant carcasses in the Tsavo (East) National Park, Kenya.

559   *J. Arid Environ.,* 1, 71–86, https://doi.org/10.1016/S0140-1963(18)31756-7, 1978.

560   21. Coetsee, M. & Ferreira, S. Bridging science, management, and opinion: GLTFCA elephant

561   management [Conference presentation]. Savanna Science Network Meeting, Skukuza,

562   Kruger National Park, South Africa, 2023 March 5-9.

563   22. Coverdale, T. C., Kartzinel, T. R., Grabowski, K. L., Shriver, R. K., Hassan, A. A., Goheen,

564   J. R., Palmer, T. M., & Pringle, R. M. Elephants in the understory: opposing direct and

565   indirect effects of consumption and ecosystem engineering by megaherbivores. *Ecol.,* 97,

566   3219–3230, https://doi.org/10.1002/ecy.1557, 2016.

567   23. Craine, J. M., Morrow, C., & Stock, W. D. Nutrient concentration ratios and co-limitation in

568   South African grasslands. *New Phytol.,* 179, 829–836, https://doi.org/10.1111/j.1469-

569   8137.2008.02513.x, 2008.

570   24. Croghan C. & Egeghy P. P., Methods of dealing with values below the limit of detection

571   using SAS. *Southern SAS User Group,* 22, 2003.

572   25. Danell, K., Berteaux, D., & Bråthen, K. A. Effect of muskox carcasses on nitrogen

573   concentration in tundra vegetation. *Arctic*, 55, 389–392, http://www.jstor.org/stable/40512497,

574   2002.

575   26. Davies, A. B., Levick, S. R., Robertson, M. P., van Rensburg, B. J., Asner, G. P. & Parr, C.

576   L. Termite mounds differ in their importance for herbivores across savanna types, seasons

577   and spatial scales. *Oikos*, 125, 726-734, https://doi.org/10.1111/oik.02742, 2016.

578   27. Doughty, C. E., Roman, J., Faurby, S., Wolf, A., Haque, A., Bakker, E. S., Malhi, Y.,

579   Dunning, J. B., Jr, & Svenning, J.-C. Global nutrient transport in a world of giants. *PNAS,*

580   113, 868–873, https://doi.org/10.1073/pnas.1502549112, 2016.

581   28. Doughty, C. E., Wolf, A., & Malhi, Y. The legacy of the Pleistocene megafauna extinctions

582   on nutrient availability in Amazonia. *Nat. Geosci.,* 6, 761–764,

583   https://doi.org/10.1038/ngeo1895, 2013.

584   29. Epron, D., Laclau, J-P., Almeida, J. C. R., Gonçalves, J. L. M., Ponton, S., Sette, Jr., C. R.,

585   Delgado-Rojas, J. S., Bouillet, J-P. & Nouvellon, Y. Do changes in carbon allocation account

586   for the growth response to potassium and sodium applications in tropical Eucalyptus

587   plantations? *Tree Physiology*, 32, 667-679, https://doi.org/10.1093/treephys/tpr107, 2012.

588   30. Esala, M. J. Changes in the extractable ammonium- and nitrate-nitrogen contents of soil

589   samples during freezing and thawing. *Commun. Soil Sci. Plant Anal.*, 26, 61-68,

590   https://doi.org/10.1080/00103629509369280, 1995.

591   31. FAO. Standard operating procedure for soil available phosphorus - Bray I and Bray II

592   method. http://www.fao.org/3/cb3460en/cb3460en.pdf, 2021.

593   32. Flannery, T. F. Pleistocene faunal loss: implications of the aftershock for Australia's past and

594   future. *Archaeol. Ocean.*, 25, 45–55, https://doi.org/10.1002/j.1834-4453.1990.tb00232.x,

595   1990.

596   33. Gertenbach, W. Landscapes of the Kruger National Park. *Koedoe*, 26, 9-121,

597   https://doi.org/10.4102/koedoe.v26i1.591, 1983.

598   34. Goldenberg, S. Z. & Wittemyer, G. Elephant behavior toward the dead: A review and

599   insights from field observations. *Primates,* 61, 119-128, https://doi.org/10.1007/s10329-019-

600   00766-5, 2020.

601   35. Grant, C. C., & Scholes, M. C. The importance of nutrient hot-spots in the conservation and

602   management of large wild mammalian herbivores in semi-arid savannas. *Biol. Conserv.,* 130,

603   426–437, https://doi.org/10.1016/j.biocon.2006.01.004, 2006.

604   36. Gray, E. F. & Bond, W. Soil nutrients in an African forest/savanna mosaic: Drivers or

605   driven? *S. Afr. J. Bot.,* 101, 66-72, https://doi.org/10.1016/j.sajb.2015.06.003, 2015.

606   37. Guy, T. J., Hutchinson, M. C., Baldock, K. C. R., Kayser, E., Baiser, B., Staniczenko, P. P.

607   A., Goheen, J. R., Pringle, R. M., & Palmer, T. M. Large herbivores transform plant-

608   pollinator networks in an African savanna. *Curr. Biol.,* 2964–2971,

609   https://doi.org/10.1016/j.cub.2021.04.051, 2021.

610   38. Hocking, M. D. & Reynolds, J. D. Nitrogen uptake by plants subsidized by Pacific salmon

611   carcasses: a hierarchical experiment. *Can. J. For. Res.,* 42, 908-917,

612   https://doi.org/10.1139/x2012-045, 2012.

613   39. Holdo, R. M. Effects of fire history and N and P fertilization on seedling biomass, specific

614   leaf area, and root:shoot ratios in a South African savannah. *S. Afr. J. Bot.*, 86, 5–8,

615   https://doi.org/10.1016/j.sajb.2013.01.005, 2013.

616   40. Holdo, R. M. & Mack, M. C. Functional attributes of savanna soils: contrasting effects of

617   tree canopies and herbivores on bulk density, nutrients and moisture dynamics. *J. Ecol.,* 102,

618   1171-1182, https://doi.org/10.1111/1365-2745.12290, 2014.

619   41. Hu, L., Wu, Z., Robert, C. A. M., Ouyang, X., Züst, T., Mestrot, A., Xu, J., & Erb, M. Soil

620   chemistry determines whether defensive plant secondary metabolites promote or suppress

621   herbivore growth. *PNAS*, 118, e2109602118, https://doi.org/10.1073/pnas.2109602118,

622   2021.

623   42. Joern, A., Provin, T., & Behmer, S. T. Not just the usual suspects: insect herbivore

624   populations and communities are associated with multiple plant nutrients. *Ecol.,* 93, 1002–

625   1015, https://doi.org/10.1890/11-1142.1, 2012.

626   43. Kaspari, M. The invisible hand of the periodic table: how micronutrients shape ecology.

627   *Annu. Rev. Ecol. Evol. Syst.,* 52, 199–219, https://doi.org/10.1146/annurev-ecolsys-012021-

628   090118, 2021.

629   44. Keenan, S. W., Schaeffer, S. M., Jin, V. L. & DeBruyn, J. M. Mortality hotspots: nitrogen

630   cycling in forest soils during vertebrate decomposition. *Soil Biol. Biochem.,* 121, 165-176,

631   https://doi.org/10.1016/j.soilbio.2018.03.005, 2018.

632   45. Keenan, S. W., Schaeffer, S. M., and DeBruyn, J. M. Spatial changes in soil stable isotopic

633   composition in response to carrion decomposition. *Biogeosciences,* 16, 3929–3939,

634   https://doi.org/10.5194/bg-16-3929-2019, 2019.

635   46. Keenan, S. W., & Beeler, S. R. Long-term effects of buried vertebrate carcasses on soil

636   biogeochemistry in the Northern Great Plains. *PloS One*, 18, e0292994,

637   https://doi.org/10.1371/journal.pone.0292994, 2023.

638 47. Khomo, L., Trumbore, S., Bern, C. R. & Chadwick, O. A. Timescales of carbon turnover in

639   soils with mixed crystalline mineralogies. *SOIL*, 3, 17-30, https://doi.org/10.5194/soil-3-17-

640   2017, 2017.

641 48. Lathwell, D. J. & Grove, T. L. Soil-plant relationships in the tropics. *Annu. Rev. Ecol. Syst.*,

642   17, 1-16, https://www.jstor.org/stable/2096986, 1986.

643 49. Lemoine, N. P., Budny, M. L., Rose, E., Lucas, J., & Marshall, C. W. Seasonal soil moisture

644   thresholds inhibit bacterial activity and decomposition during drought in a tallgrass prairie.

645   *Oikos*, 2024, e10210, https://doi.org/10.1111/oik.10201, 2023.

646 50. Macdonald, B. C. T., Farrell, M., Tuomi, S., Barton, P. S., Cunningham, S. A., & Manning,

647   A. D. Carrion decomposition causes large and lasting effects on soil amino acid and peptide

648   flux. *Soil Biol. Biochem.*, 69, 132–140, https://doi.org/10.1016/j.soilbio.2013.10.042, 2014.

649 51. Moleón, M., Sánchez-Sapata, J. A., Sebastián-González, E. & Owen-Smith, N. Carcass size

650   shapes the structure and functioning of an African scavenging assemblage. *Oikos,* 124, 1391-

651   1403, https://doi.org/10.1111/oik.02222, 2015.

652 52. Monk, J. D., Donadio, E., Smith, J. A., Perrig, P. L., Middleton, A. D., & Schmitz, O. J.

653   Predation and biophysical context control long-term carcass nutrient inputs in an Andean

654   ecosystem. *Ecosyst.*, 27, 346–359, https://doi.org/10.1007/s10021-023-00893-7, 2024.

655 53. Morris, A. W., Smith, I., Chakrabarti, S., Lala, F., Nyaga, S. & Bump, J. K. Eating an

656   elephant, one bite at a time: predator interactions at carrion bonanzas. *Food Webs*, 37,

657   e00304, https://doi.org/10.1016/j.fooweb.2023.e00304, 2023.

658 54. Mphepya, J. N., Galy-Lacaux, C., Lacaux, J. P., Held, G., & Pienaar, J. J. Precipitation

659   chemistry and wet deposition in Kruger National Park, South Africa. *J. Atmos. Chem.*, 53,

660   169–183, https://doi.org/10.1007/s10874-005-9005-7, 2006.

661   55. Oksanen J, Simpson G, Blanchet F, Kindt R, Legendre P, Minchin P, O'Hara R, Solymos P,

662   Stevens M, Szoecs E, Wagner H, Barbour M, Bedward M, Bolker B, Borcard D, Carvalho G,

663   Chirico M, De Caceres M, Durand S, Evangelista H, FitzJohn R, Friendly M, Furneaux B,

664   Hannigan G, Hill M, Lahti L, McGlinn D, Ouellette M, Ribeiro Cunha E, Smith T, Stier A,

665   Ter Braak C, Weedon J. Community Ecology Package. R package version 2.6-4,

666   https://CRAN.R-project.org/package=vegan, 2022.

667   56. Olea, P.P, Mateo-Tomas, P., Sanchez-Zapata, J.A. (eds.) Carrion Ecology and Management.

668   Springer, NY, USA, 2019.

669   57. Owen-Smith, N. Megafaunal extinctions: the conservation message from 11,000 years B.P.

670   *Conserv. Biol.,* 3, 405–412, https://www.jstor.org/stable/2386221, 1989.

671   58. Owen-Smith, N., & Mills, M. G. L. Predator-prey size relationships in an African large-

672   mammal food web. *J. Anim. Ecol.,* 77, 173–183, https://doi.org/10.1111/j.1365-

673   2656.2007.01314.x, 2008.

674   59. Pandey, N. Role of micronutrients in reproductive physiology of plants. *Plant Stress*, 4, 1-13.

675   https://www.semanticscholar.org/paper/af9a8662b83613f6e0d5e538ed33f3add4a1d5a1,

676   2010.

677   60. Parmenter, R. R., & MacMahon, J. A. Carrion decomposition and nutrient cycling in a

678   semiarid shrub–steppe ecosystem. *Ecol. Monogr*., 79, 637–661, https://doi.org/10.1890/08-

679   0972.1, 2009.

680   61. Pellegrini, A. F. A. Nutrient limitation in tropical savannas across multiple scales and

681   mechanisms. *Ecol*., 97, 313–324, https://doi.org/10.1890/15-0869.1, 2016.

682   62. Prosser, J. I. Soil Nitrifiers and Nitrification. In Nitrification. ASM Press, pp. 347-383, 2014.

683   63. Quaggiotto, M.-M., Evans, M. J., Higgins, A., Strong, C., & Barton, P. S. Dynamic soil

684   nutrient and moisture changes under decomposing vertebrate carcasses. *Biogeochemistry*,

685   146, 71–82, https://doi.org/10.1007/s10533-019-00611-3, 2019.

686   64. R Core Team. R: A language and environment for statistical computing. R Foundation for

687   Statistical Computing, Vienna, Austria. https://www.R-project.org/, 2022.

688   65. Ries, L. P., & Shugart, H. H. Nutrient limitations on understory grass productivity and

689   carbon assimilation in an African woodland savanna. *J. Arid Environ*., 72, 1423–1430,

690   https://doi.org/10.1016/j.jaridenv.2008.02.013, 2008.

691   66. Ripple, W. J., Newsome, T. M., Wolf, C., Dirzo, R., Everatt, K. T., Galetti, M., Hayward, M.

692   W., Kerley, G. I. H., Levi, T., Lindsey, P. A., Macdonald, D. W., Malhi, Y., Painter, L. E.,

693   Sandom, C. J., Terborgh, J., & Van Valkenburgh, B. Collapse of the world's largest

694   herbivores. *Sci. Adv.,* 1, e1400103, https://doi.org/10.1126/sciadv.1400103, 2015.

695   67. Risch, A. C., Frossard, A., Schütz, M., Frey, B., Morris, A. W., & Bump, J. K. Effects of elk

696   and bison carcasses on soil microbial communities and ecosystem functions in Yellowstone,

697   USA. *Funct. Ecol.,* 34, 1933–1944, https://doi.org/10.1111/1365-2435.13611, 2020.

698   68. Roman, J., Estes, J. A., Morissette, L., Smith, C., Costa, D., McCarthy, J., Nation, J. B.,

699   Nicol, S., Pershing, A., & Smetacek, V. *Whales as marine ecosystem engineers. Front. Ecol.*

700   *Environ.,* 12, 377–385, https://doi.org/10.1890/130220, 2014.

701   69. Rughöft, S., Hermann, M., Lazar, C. S., Cesarz, S., Levick, S. R., Trumbore, S. E. & Küsel,

702   K. Community composition and abundance of bacterial, archaeal and nitrifying populations

703   in savanna soils on contrasting bedrock material in Kruger National Park, South Africa.

704   *Front. Microbiol.,* 7, https://doi.org/10.3389/fmicb.2016.01638, 2016.

705   70. Sardans, J., & Peñuelas, J. Potassium control of plant functions: ecological and agricultural

706   implications. *Plants*, 10, https://doi.org/10.3390/plants10020419, 2021.

707   71. Schmitz, O. J., Wilmers, C. C., Leroux, S. J., Doughty, C. E., Atwood, T. B., Galetti, M.,

708   Davies, A. B., & Goetz, S. J. Animals and the zoogeochemistry of the carbon cycle. *Science*,

709   362, https://doi.org/10.1126/science.aar3213, 2018.

710   72. Seymour, C. L., Milewski, A. V., Mills, A. J., Joseph, G. S., Cumming, G. S., Cumming, D.

711   H. M. & Mahlangu, Z. Do the large termite mounds of *Macrotermes* concentrate

712   micronutrients in addition to macronutrients in nutrient-poor African savannas? *Soil Biology*

713   *and Biogeochemistry*, 68, 95-105, https://doi.org/10.1016/j.soilbio.2013.09.022, 2014.

714   73. Skarpe, C., Aarrestad, P. A., Andreassen, H. P., Dhillion, S. S., Dimakatso, T., du Toit, J. T.,

715   Duncan, Halley, J., Hytteborn, H., Makhabu, S., Mari, M., Marokane, W., Masunga, G.,

716   Ditshoswane, M., Moe, S. R., Mojaphoko, R., Mosugelo, D., Motsumi, S., Neo-Mahupeleng,

717   G., … Wegge, P. The return of the giants: ecological effects of an increasing elephant

718   population. *Ambio*, 33, 276–282, http://www.jstor.org/stable/4315497, 2004.

719   74. Sollen-Norrlin, M. & Rintoul-Hynes, N. L. J. Soil sample storage conditions affect

720   measurements of pH, potassium, and nitrogen. *SSSAJ*, 88, 930-941,

721   https://doi.org/10.1002/saj2.20653, 2024.

722   75. Sonneveld, C. & van den Ende, J. Soil analysis by means of a 1:2 volume extract. Plant and

723   Soil, 63, 523-526, https://www.jstor.org/stable/42933277, 1971.

724   76. Sterner, R. W., & Elser, J. J. Ecological Stoichiometry: The Biology of Elements from

725   Molecules to the Biosphere. Princeton University Press.

726   http://www.jstor.org/stable/j.ctt1jktrp3, 2002.

727   77. Subalusky, A. L., Dutton, C. L., Rosi, E. J., & Post, D. M. Annual mass drownings of the

728   Serengeti wildebeest migration influence nutrient cycling and storage in the Mara River.

729   *PNAS*, 114, 7647–7652, https://doi.org/10.1073/pnas.1614778114, 2017.

730   78. Subalusky, A.L., Dutton, C.L., Rosi, E.J, Puth, L.M., Post, D.M. River of bones: wildebeest

731   skeletons leave a legacy of mass mortality in Mara River, Kenya. *Front. Ecol. Evol.,* 8,

732   https://doi.org/10.3389/fevo.2020.00031, 2020.

733   79. Towne, E. G. Prairie vegetation and soil nutrient responses to ungulate carcasses. *Oecologia*,

734   122, 232–239, https://www.jstor.org/stable/4222536, 2000.

735   80. Turner, B. L. & Romero, T. E. Short-term changes in extractable inorganic nutrients during

736   storage of tropical rainforest soils. *SSSAJ*, 73, 1972-1979,

737   https://doi.org/10.2136/sssaj2008.0407, 2009.

738   81. Turner, W. C., Kausrud, K. L., Krishnappa, Y. S., Cromsigt, J. P. G. M., Ganz, H. H.,

739   Mapaure, I., Cloete, C. C., Havarua, Z., Küsters, M., Getz, W. M., & Stenseth, N. C. Fatal

740   attraction: vegetation responses to nutrient inputs attract herbivores to infectious anthrax

741   carcass sites. *Proc. R. Soc. B*, 281, https://doi.org/10.1098/rspb.2014.1785, 2014.

742   82. van Klink, R., van Laar-Wiersma, J., Vorst, O., & Smit, C. Rewilding with large herbivores:

743   Positive direct and delayed effects of carrion on plant and arthropod communities. *PloS One*,

744   15, e0226946, https://doi.org/10.1371/journal.pone.0226946, 2020.

745   83. Venter, F. J., Scholes, R. J. & Eckhardt, H. C. Abiotic template and its associated vegetation

746   pattern. In: J. T. Du Toit, K. H. Rogers, H. C. Biggs, eds. The Kruger experience: ecology

747   and management of savanna heterogeneity. Washington, DC, USA: Island Press, 83–129,

748   2003.

749   84. Wiersum, L. K. Uptake of nitrogen and phosphorus in relation to soil structure and nutrient

750   mobility. *Plant Soil,* 16, 62–70, https://doi.org/10.1007/BF01378158, 1962.

751   85. Wigley, B. J., Coetsee, C., Fritz, C. & Bond, W. J. Herbivores shape woody plant

752   communities in the Kruger National Park: lessons from three long-term exclosures: original

753   research. *Koedoe*, 56, http://dx.doi.org/10.4102/koedoe.v56i1.1165, 2014.

754   86. Yang, L. H. Periodical cicadas as resource pulses in North American forests. *Science*, 306,

755   1565–1567, https://doi.org/10.1126/science.1103114, 2004.

756   87. Yang, L. H. Pulses of dead periodical cicadas increase herbivory of American bellflowers.

757   *Ecol.,* 89, 1497–1502, https://doi.org/10.1890/07-1853.1, 2008.

758   88. Yong, S. K., Jalaludin, N. H., Brau, E., Shamsudin, N. N., & Heo, C. C. Changes in soil

759   nutrients (ammonia, phosphate and nitrate) associated with rat carcass decomposition under

760   tropical climatic conditions. *Soil Res*., 57, 482–488, https://doi.org/10.1071/SR18279, 2019.
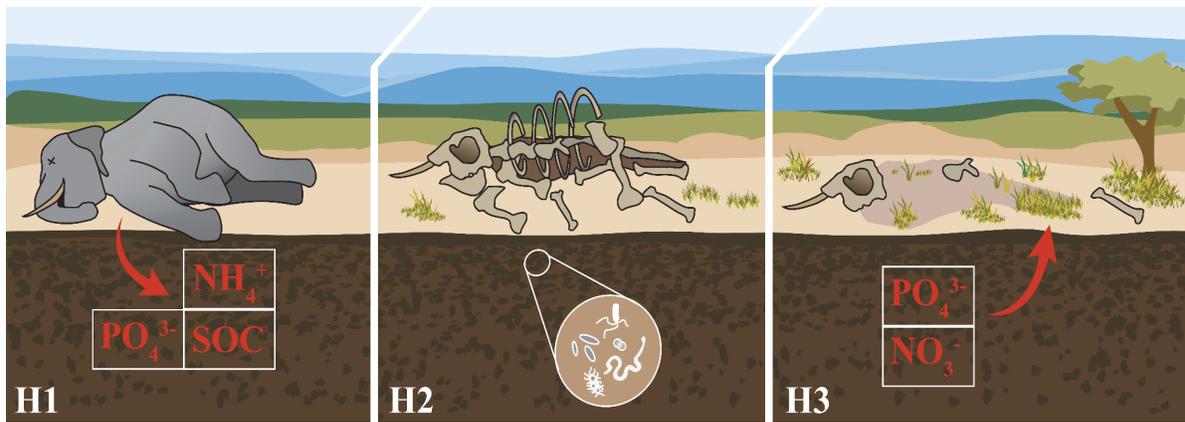
Figure 1. Hypothesized impacts of elephant megacarcasses on soil and plant nutrients. First (H1), we hypothesized that elephant carcasses would release pulses of nutrients into the soil, resulting in higher concentrations of soil ions such as nitrogen (ammonium, $[NH_4]^+$), phosphorus (phosphate, $[PO_4]^{3-}$), and soil organic C. Second (H2), we hypothesized that C inputs from the carcass would result in increased soil microbial respiration potential. Third (H3), we hypothesized that plants would take up nutrients from the carcass soil, resulting in plants with distinct nutrient profiles and increased concentrations of key limiting nutrients such as N and P. Image credit: Kirsten Boeh.
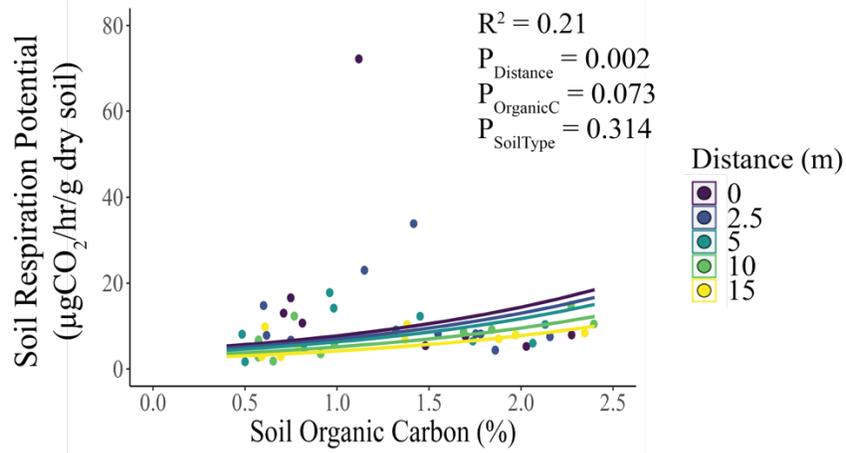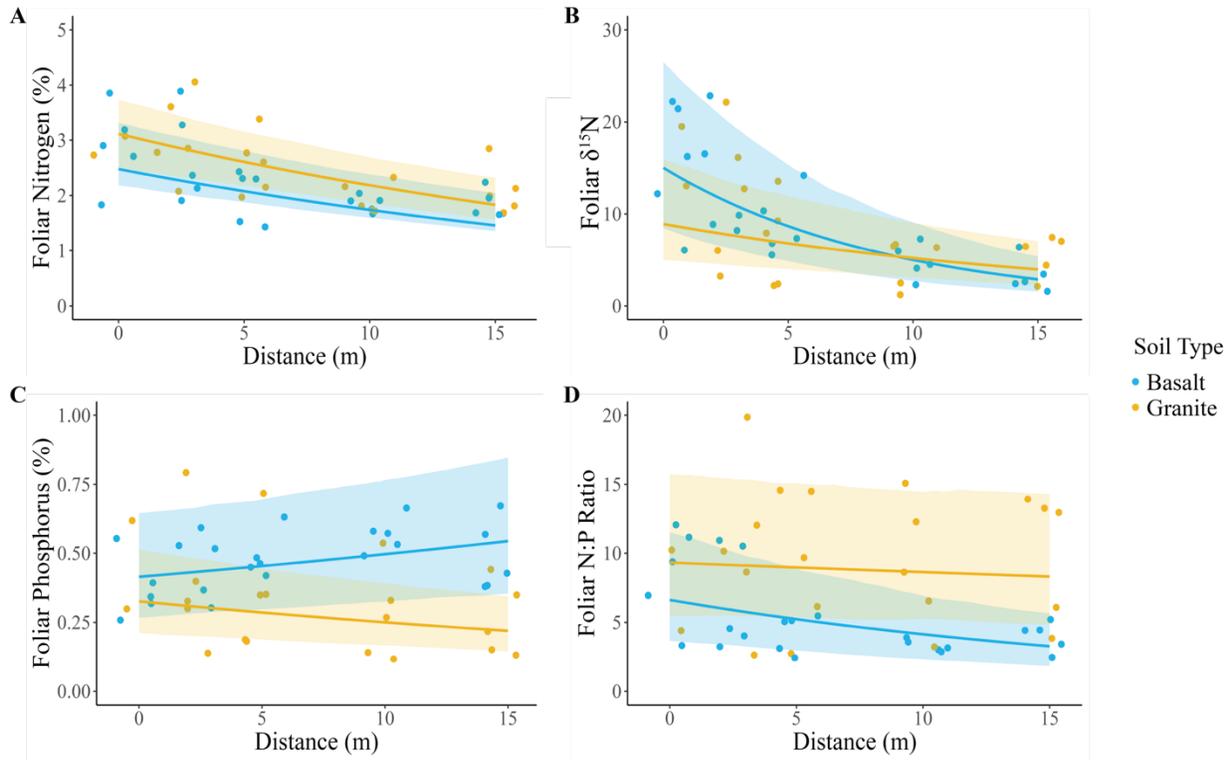
770
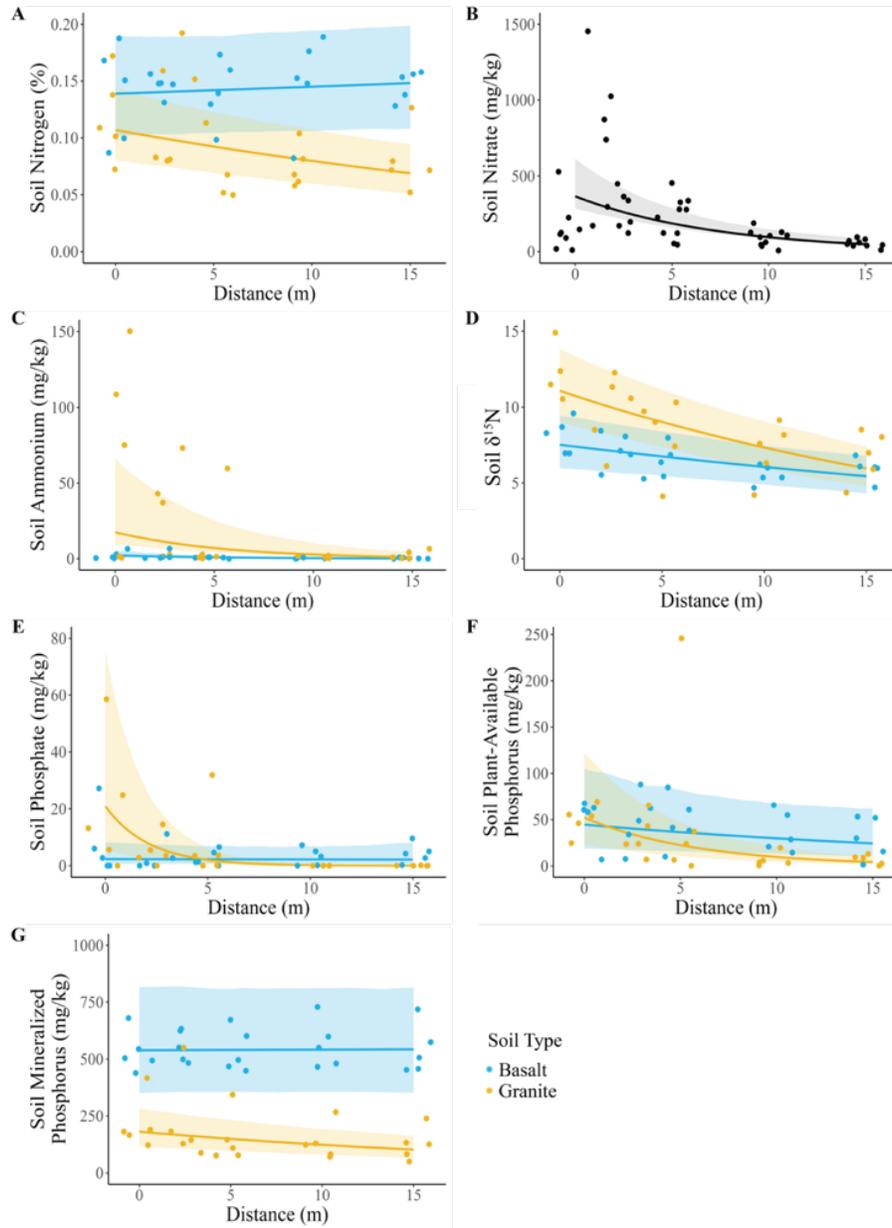
Figure 2. Effects of elephant carcasses on soil N and P concentrations in granitic and basaltic

soils. (A) Soil N (%) was greater in basaltic soils, and in granitic soils it decreased with distance

from the carcass site. (B) Soil nitrate nitrogen decreased with distance but did not differ between

soil types. (C) Soil ammonium nitrogen and (D) $\delta^{15}N$ were both greater in granitic soils and

decreased with distance from the carcass. (E) Soil phosphate, (F) plant-available P, and (G)

mineralized P decreased with distance in granitic soils but not basaltic soils. Points represent

777   individual measurements from soil samples taken at 0, 2.5, 5, 10, and 15m and are offset to be

778   visible when they would otherwise overlap. Lines show predictions calculated from the top

779   generalized linear mixed model, which may include soil type, distance, and soil type by distance

780   interaction as covariates (Table S1). Only significant relationships are shown on plots. Shading

781   indicates the 95% confidence interval.

The plot shows Soil Respiration Potential (μgCO_2/hr/g dry soil) on the y-axis (0 to 80) versus Soil Organic Carbon (%) on the x-axis (0.0 to 2.5).

$R^2 = 0.21$
$P_{Distance} = 0.002$
$P_{OrganicC} = 0.073$
$P_{SoilType} = 0.314$

Distance (m)
0
2.5
5
10
15

Figure 3. Effects of elephant carcasses on soil respiration potential. We regressed soil respiration against soil organic carbon, with distance and soil type as covariates. Soil respiration potential was marginally positively correlated with soil organic C (%) and decreased significantly with distance from the carcass. Points represent individual measurements taken from soil samples at 0, 2.5, 5, 10, and 15m and are offset to be visible when they would otherwise overlap. Lines represent model predictions. Only significant relationships are shown.

Figure 4. Effects of elephant carcasses on foliar N and P concentrations in granitic and basaltic soils. (A) Foliar %N was higher in granitic soils and decreased with distance from the carcass center. (B) Foliar $\delta^{15}N$ decreased with distance from the carcass center and exhibited a significant interaction in which $\delta^{15}N$ decreased more rapidly with distance in basaltic soils. (C) Foliar P was greater in basaltic soils and decreased with distance in granitic soils. (D) Foliar N:P ratio was greater in granitic soils and decreased with distance from the carcass center for both soil types. Points represent individual measurements from soil samples taken at 0, 2.5, 5, 10, and 15m and are offset to be visible when they would otherwise overlap. Lines show predictions calculated from the top generalized linear mixed model, which may include soil type, distance, and soil type by distance interaction as covariates (Table S2). Only significant relationships are shown on plots. Shading indicates the 95% confidence interval. Three of the ten sites had bare ground at the 0 m distance, resulting in a sample size of 7 sites for that distance and 10 for the other distances.

803
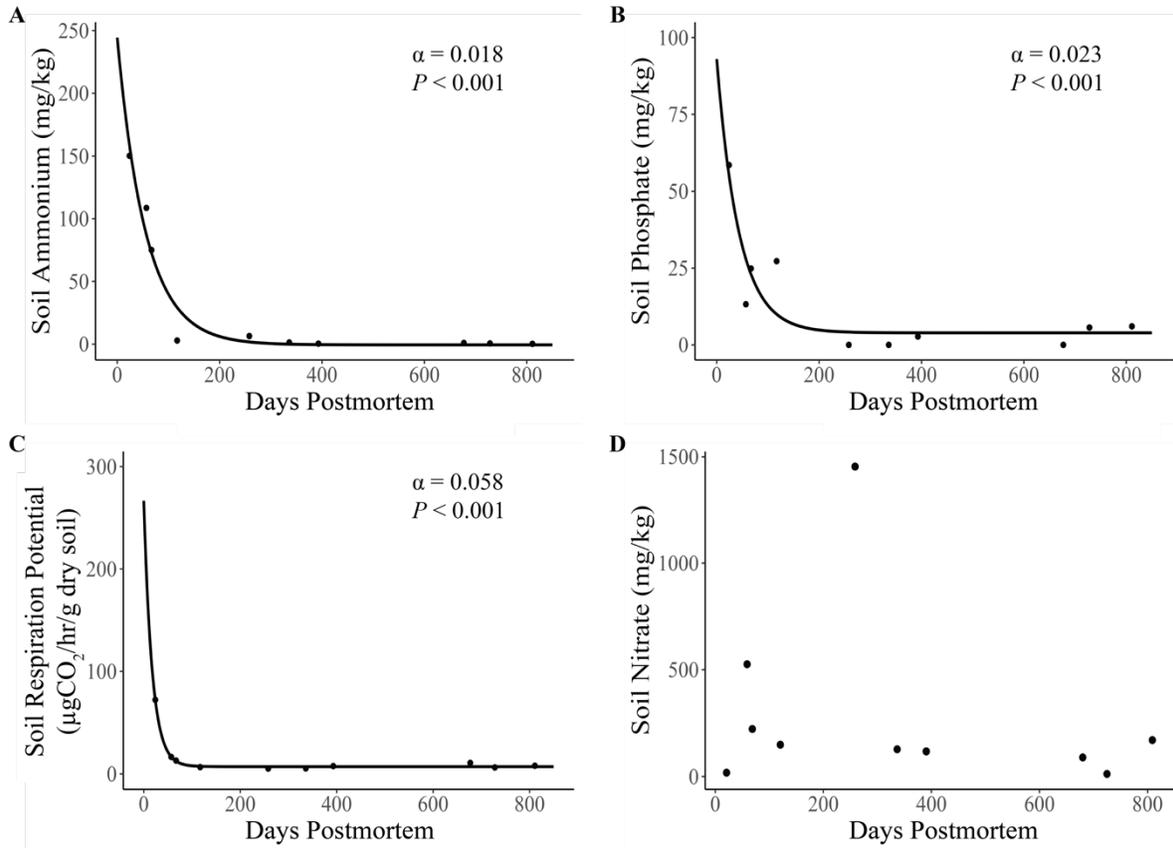
Figure 5. Relationship between carcass age and key soil metrics (soil ion concentrations and respiration potential). Lines represent predictions from exponential decay models, with α equal to the rate of decay. (A) Soil ammonium, (B) phosphate, and (C) respiration potential all decreased significantly with carcass age. The model for (D) soil nitrate failed to converge. Points represent individual measurements taken at the center of the carcass site (distance = 0.5m). Only significant relationships are shown on plots.